Tuning the Dipole-Dipole Interaction in a Quantum Gas with a Rotating Magnetic Field

Yijun Tang, Wil Kao, Kuan-Yu Li, and Benjamin L. Lev

Phys. Rev. Lett. **120**, 230401 — Published 4 June 2018

DOI: 10.1103/PhysRevLett.120.230401

Tuning the dipole-dipole interaction in a quantum gas with a rotating magnetic field

Yijun Tang,[1,2] Wil Kao,[2,3] Kuan-Yu Li,[2,3] and Benjamin L. Lev[1,2,3]

[1]*Department of Physics, Stanford University, Stanford CA 94305*
[2]*E. L. Ginzton Laboratory, Stanford University, Stanford CA 94305*
[3]*Department of Applied Physics, Stanford University, Stanford CA 94305*

(Dated: April 30, 2018)

We demonstrate the tuning of the magnetic dipole-dipole interaction (DDI) within a dysprosium Bose-Einstein condensate by rapidly rotating the orientation of the atomic dipoles. The tunability of the dipolar mean-field energy manifests as a modified gas aspect ratio after time-of-flight expansion. We demonstrate that both the magnitude and the sign of the DDI can be tuned using this technique. In particular, we show that a magic rotation angle exists at which the mean-field DDI can be eliminated, and at this angle, we observe that the expansion dynamics of the condensate is close to that predicted for a non-dipolar gas. The ability to tune the strength of the DDI opens new avenues toward the creation of exotic soliton and vortex states as well as unusual quantum lattice phases and Weyl superfluids.

Recent advancements in laser cooling and trapping of highly magnetic lanthanide atoms such as dysprosium and erbium have introduced strong magnetic dipole-dipole interactions (DDI) into the toolbox of ultracold atomic physics [1–4]. When paired with the short-ranged Van der Waals s-wave interaction, the long-ranged and anisotropic DDI dramatically modifies the atomic gas properties and has enabled the exploration of a wide variety of phenomena. These range from novel quantum liquids [5–8] and strongly correlated lattice states [9–11], to exotic spin dynamics [12, 13] and the emergence of thermalization in a nearly integrable quantum gas [14].

An even wider array of physics could be explored were one able to control the dipolar strength independent of the relative orientation of the dipoles. For example, exotic multidimensional bright and dark dipolar solitons could be observed [15–17] as well as exotic vortex lattices, dynamics, and interactions [18–20]. Magnetorotons in spinor condensates [21] and the nematic susceptibility of dipolar Fermi gases [22–25] could be controlled by tuning the strength of the DDI. In optical lattices, one would be able to create tunable dipolar Luttinger liquids [26, 27] as well as novel quantum phases [28], including analogs of fractional quantum Hall states [29]. Intriguingly, Weyl superfluidity may be observable in dipolar Fermi gases by tuning the DDI [30]. Tuning the DDI in 2D dipolar Bose-Einstein condensates (BECs) may allow for the probing of scale invariance in analogs of inflationary cosmology [31]. Setting the DDI strength to zero has application in improving the sensitivity of atom interferometers [32], while tuning the strength negative may find application in the simulation of dense nuclear matter through analogies with the tensor nuclear force [33].

We realize a method, first proposed for quantum gases in 2002 [34][35], to tune the DDI strength from positive to zero, and even to negative values. Although the static DDI between two spin-polarized atoms cannot be tuned, the time-averaged DDI can be tuned by quickly rotating the dipoles. This provides control of the ratio ϵ of the dipolar mean-field energy to the mean-field contact energy without the use of a Feshbach resonance to control a_s, the s-wave scattering length [36][37]. This ratio is $\epsilon = \mu_0\mu^2 m/12\pi\hbar^2 a_s$, where μ is the magnetic moment, m is the mass, and μ_0 is the permeability of free space. The attractive component of the DDI can lead to dipolar collapse: $\epsilon = 1$ demarcates the boundary between mechanically stable and unstable homogeneous condensates at the mean-field level [17].

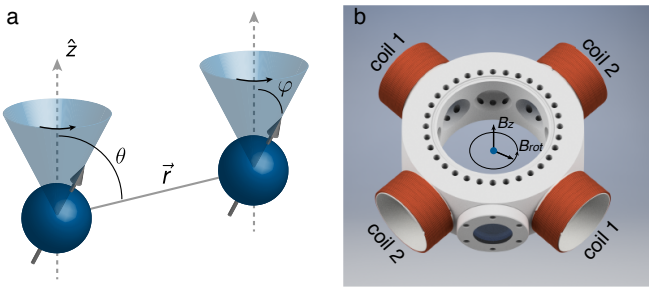

FIG. 1. Tuning the DDI strength by rotating the magnetic dipoles. (a) Geometry of the rotating field technique. The dipoles are rotated along a cone centered around the $\hat{z}$ direction. (b) Schematic showing the trapping chamber and the two pairs of coils used for generating the rotating component of the magnetic field. Sizes are drawn to scale; diameter of coils is 7 cm. The coils for generating $\hat{z}$ field and other vacuum chamber parts are not shown. The atoms are located at the center of the chamber.

Figure 1(a) illustrates the geometry of the rotating dipoles. A rotating magnetic field in the $\hat{x}$-$\hat{y}$ plane causes the dipoles to rotate at an angle φ with respect to a static magnetic field along the $\hat{z}$-axis. Assuming cylindrically symmetric trap frequencies $\omega_x = \omega_y$ for simplicity, the time-averaged DDI between two atoms is [34]

$$\langle U_{\mathrm{DDI}}(\mathbf{r},\theta,\varphi)\rangle = -\frac{\mu_0\mu^2}{4\pi}\left(\frac{3\cos^2\theta-1}{|\mathbf{r}|^3}\right)\left(\frac{3\cos^2\varphi-1}{2}\right), \quad (1)$$

where $\mathbf{r}$ is the relative position vector between the two

atoms, θ is the angle between $\mathbf{r}$ and $\hat{z}$, and $\mu = 9.93\mu_B$ is the magnetic dipole moment for ^{162}Dy, the species of atom employed for this work [38]. This time-averaged DDI is simply the regular DDI modified by the term in the second parentheses. This term changes from 1 to -0.5 as φ is tuned from 0° to 90° by changing the ratio of the rotation to static field strengths. This enables the tuning of both the magnitude and the sign of the DDI. For $\varphi > \varphi_m$, even atoms sitting side-by-side experience an attractive averaged DDI due to the inversion of their dipoles by the rotating field. Moreover, the DDI vanishes for any θ, i.e., any pair of atoms in the gas, at the so-called magic angle $\varphi_m = 54.7°$. We note that an alternative method for reducing the strength of the DDI—spin-polarizing in $|m_F| < F$ Zeeman substates—unfortunately leads to gas heating and/or atom loss from dipolar relaxation [39–41].

In this work, we prepare ^{162}Dy BECs with $2.0(2) \times 10^4$ atoms in the absolute ground Zeeman sublevel $m_J = -8$ ($J = 8$). The BECs are created by evaporative cooling in crossed 1064-nm optical dipole traps (ODT). The procedure is similar to that described in a previous publication [42]. The present experiment differs only in that instead of loading atoms from the magneto-optical trap using a spatially dithered circular ODT beam, we now use a stationary elliptical ODT with a horizontal waist of 73(3) μm and a vertical waist of 19(2) μm.

The rapid rotation of the atomic dipoles is realized by rotating a bias magnetic field at $\omega_r = 2\pi \times 1$ kHz. This is chosen to be fast compared to the trap frequencies $[\omega_x,\omega_y,\omega_z] = 2\pi\times[73(1),37(2),74(1)]$ Hz to avoid parametric heating, but is slow compared to the Larmor frequency 1.55 MHz to ensure that the rotation is adiabatic. The rotating field consists of a static component along $\hat{z}$ and a rotating component in the x-y plane generated by a pair of coils driven 90° out-of-phase using two bipolar current sources, as illustrated in Fig. 1(b). The total field as a function of time t can be written as $\mathbf{B}(t) = B_{\rm rot}\left[\cos(\omega_r t + \pi/4)\hat{x} + \sin(\omega_r t + \pi/4)\hat{y}\right] + B_z\hat{z}$, where the total magnitude $B = \sqrt{B_{\rm rot}^2 + B_z^2}$ is fixed at 0.89(2) G [43], away from any Feshbach resonances [44], and the rotation angle is related to the magnitude of the two components by $\tan\varphi = B_{\rm rot}/B_z$. The vertical field B_z is provided by a pair of coils in the $\hat{z}$ direction and is not shown in Fig. 1(b). The angle φ is controlled using a calibration procedure that corrects for the effect of eddy currents. We now describe the calibration.

Because the coils generating the rotating component of the field are mounted outside the stainless steel vacuum chamber, the magnitude of the rotating component $B_{\rm rot}$ is reduced due to eddy currents compared to a static field B_s generated by driving the coils with the equivalent DC current. We calibrate the effect of eddy currents by measuring $B_{\rm rot}$ at different B_s. The field magnitude is measured using rf-spectroscopy, where we drive the atoms with a single-tone rf-field at frequency $\omega_{\rm rf}$. When

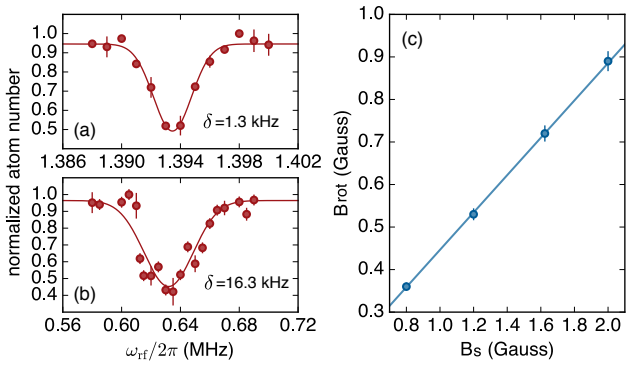

FIG. 2. (a) Atom-loss spectrum from a rf-spectroscopy measurement at a DC field $B_s = 0.802$ G. (b) Atom-loss spectrum from a rf-spectroscopy measurement for a rotating field $B_{\rm rot}$ generated with AC current of the same amplitude. The resonance shifts to a lower frequency due to effects of eddy currents. The resonance width increases from 1.3 kHz (0.7 mG) to 16.3 kHz (9.4 mG) due to residual fluctuations of the rotating field amplitude. (c) Measured linear dependence between $B_{\rm rot}$ and B_s. Error bars represent one standard error.

$\omega_{\rm rf}$ matches the Zeeman splitting, the atoms are transferred to higher Zeeman states and subsequently dipolar relax. This causes rapid atom loss, which heralds the resonance [39–41]. The Zeeman splitting is 1.7378 MHz/G for bosonic dysprosium [45]. The atom loss spectra of a typical set of rotating $B_{\rm rot}$ and static B_s fields are shown in Fig. 2. The magnitude of the field can be determined from the central location of the atom-loss resonance, and the stability of the field can be determined from the resonance linewidth. Figure 2(a) shows the spectrum for a static field. The resonance center is located at $\omega_{\rm rf} = 1.393$ MHz, corresponding to 0.802 G, and the linewidth, defined as the standard deviation of a Gaussian fit, is 1.3 kHz, equivalent to 0.7 mG. When the coils are driven with AC current of the same amplitude, the resulting rf-spectrum is shown in Fig. 2(b). The magnitude of this rotating field is reduced to $B_{\rm rot} = 0.364$ G by eddy currents and the linewidth is broadened to 9.4 mG. This broadening provides a measure of the field's amplitude fluctuations while the field rotates. The magnitude of the fluctuation in this case is 2.6%. We measured a total of four sets of B_s and $B_{\rm rot}$, and the results are shown in Fig. 2(c). We observe a linear dependence within this field range: $B_{\rm rot} = \alpha B_s$, where $\alpha = 0.445(6)$. By using this calibration, we are able to determine the amplitude of the AC current required to produce a given rotation angle φ.

To study the manifestation of the time-averaged DDI, we measure the change in the BEC mean-field energy due to the rotating field by observing the change in aspect ratio (AR) of the BEC. We first prepare a BEC in a static bias field along $\hat{z}$. We then ramp the currents in the $\hat{z}$-coil and coil 1 to rotate the field from $\hat{z}$ to the $\mathbf{B}(0)$ configuration, setting the initial condition for the rotating field.

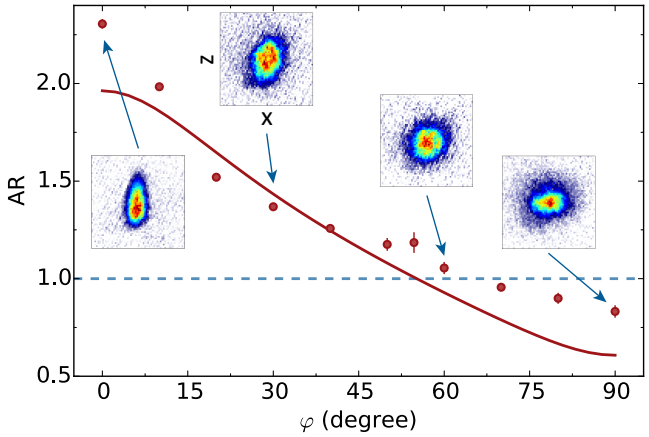

FIG. 3. Aspect ratio (AR) of the BEC after 19 ms of TOF expansion as a function of rotation angle φ. The theoretical AR, shown in solid line, is computed by solving the generalized time-dependent Gross-Pitaevskii equation [46]. Sample single-shot absorption images for $\varphi = 0°, 30°, 60°, 90°$ are shown in insets. The AR can be tuned from ∼2.3 in a static $\hat{z}$ field to below unity in a fully rotating field at $\varphi = 90°$. The $\varphi = 0°$ case corresponds to a static 1.580(5) G $\hat{z}$ field. Error bars are standard error from three measurements.

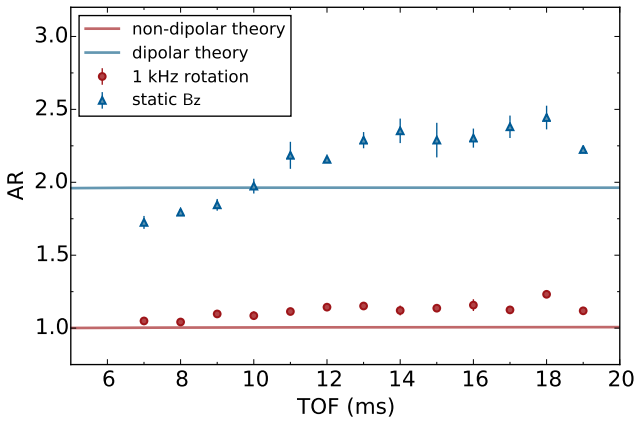

FIG. 4. AR of the BEC as a function of TOF. Triangle: expansion in a 1.580(5)-G static $\hat{z}$ field (i.e., $\varphi = 0°$). Circle: expansion in a 0.89(2) field rotating at the magic angle $\varphi_m = 54.7°$. Upper, blue line: dipolar theory prediction [46]. Lower, red line: non-dipolar theory prediction, which is equal to unity at all times for cylindrically symmetric trap parameters. The employed trap is approximately cylindrically symmetric. Error bars are standard error from three measurements.

After 10 cycles of rotation, we suddenly (in <200 μs) turn off the ODTs and let the BEC expand. We continue to rotate the fields for the first 5 ms of the time-of-flight (TOF) expansion; afterwards, the density of the atomic gas is low enough that the interactions no longer affect expansion dynamics and we can safely turn off the rotating fields without affecting the gas AR. During this first 5-ms of TOF, the gas falls 125 μm under gravity. At this displacement, the gas experiences a transverse field generated by coils 1 and 2 that is only 0.1% of the axial field: the variation of the rotation angle φ is negligible during the initial 5 ms of TOF. We then perform absorption imaging on the resonant 421-nm transition along the $\hat{y}$-direction to measure the momentum distribution in the x-z plane. We fit 1D integrated density profiles along both $\hat{x}$ and $\hat{z}$ to integrated Thomas-Fermi distributions $n(r_i) \sim [\max(1 - r_i^2/R_i^2, 0)]^2$. The AR is defined as the ratio of the extracted Thomas-Fermi radii R_z/R_x.

The AR of the BEC after 19 ms of TOF is shown in Fig. 3 for different φ. We observe that the AR monotonically decreases from ∼2.3 at $\varphi = 0°$, corresponding to a static $\hat{z}$ field where the DDI is maximally repulsive, to below unity at $\varphi = 90°$. Sample single-shot absorption images for $\varphi = 0°, 30°, 60°, 90°$ are shown in insets of Fig. 3. We note that the Thomas-Fermi radius of a non-dipolar BEC evolves in a free expansion according to $R_i(t) = \lambda_i(t)R_i(0)$, where $R_i(0)$ is the in-trap Thomas-Fermi radius and the scaling factor λ_i can be found by solving $\ddot{\lambda}_i = \omega_i^2/(\lambda_i\lambda_x\lambda_y\lambda_z)$ with initial condition $\lambda_i(0) = 1$, where $i = x, y, z$ [47]. For the trap employed in this work, we have $\omega_x \approx \omega_z$ and therefore the BEC AR should simply be equal to one in the absence of the DDI. However, the fact that AR does not equal one in our experiment is due to the DDI [17]. The observed reduction of AR with rotation angle—even to below unity—is evidence that the DDI can be tuned, as expected from Eq. (1). Also plotted is a theory curve obtained from a time-dependent Gross-Pitaevskii equation simulation generalized to include the dipolar interaction; see Refs. [46, 48, 49]. As can be seen, this mean-field treatment of the dipolar BEC expansion does not adequately fit our data. Further work must be done to extend such treatments to account for beyond mean-field effects and/or hydrodynamic effects in the early expansion [5, 50].

We also compared the evolution of AR as a function of TOF for BECs in a static field and in fields rotating at the magic angle φ_m (at which the time-averaged DDI should be zero). The results are shown in Fig. 4 for TOFs spanning 7 ms to 19 ms at 1-ms intervals. Theory predictions with and without dipolar effects are shown as well. (The generalized time-dependent Gross-Pitaevskii equation is again employed for the dipolar theory prediction [46].) The BEC gas is too dense for reliable absorption imaging earlier than 7 ms of TOF. As expected for a dipolar gas in a symmetric trap, we observe that the BEC is highly anisotropic at 7 ms of TOF in a static $\hat{z}$ field (i.e., $\varphi = 0°$). The AR asymptotes to ∼2.3. However, the AR remains near unity when expanding in a field rotating at the magic angle. This concurs with expectations for a non-dipolar BEC, suggesting that the rotating field succeeds in nearly eliminating the dipolar mean-field energy at the magic angle. Equation (1) is derived under the as-

sumption of cylindrical symmetry about $\hat{z}$: The residual deviation from unity AR may be due to the lack of this cylindrical symmetry in the trap employed.

We observed that the $1/e$ population lifetime of our BEC reached a maximum of ∼160 ms when we set the field rotation rate to be any frequency greater than a few hundred Hz, which is larger than the <100-Hz trap oscillation frequencies [51]. While this lifetime is sufficiently long for many experiments, it is one or two orders of magnitude shorter than a Dy BEC in static fields in our apparatus.

One possible explanation for the atom loss is a mechanical instability of the gas that can arise due to attractive dipolar interactions. A static magnetic field along the weakly trapped axis of a dipolar gas can lead to collapse if the attractive dipolar interaction is sufficiently strong with respect to the repulsive Van der Waals interaction [17]. It is possible that our system transiently realizes this unstable configuration when the rotating field direction swings through the weakly confined $\hat{y}$-axis. To test this possibility, we align a *static* magnetic field along the $\hat{y}$-axis. We do not observe dipolar collapse; i.e., we observe no atom loss despite the alignment of the field along the prolate axis of the gas. We conclude that the dipolar interactions are not sufficiently strong to induce atom loss.

The atom loss is more likely due to residual field gradients that lead to a parametric motional excitation associated with the rotating component $B_{\rm rot}$. As shown in Fig. 1(b), drawn to scale, the two coils are not in strict Helmholtz coil configuration, leading to non-negligible field gradients. Eddy currents in the vacuum parts could also lead to heating, but this effect cannot be controlled or separately measured in our present apparatus. We expect that by placing two pairs of orthogonal Helmholtz coils inside vacuum, or outside a glass cell, one could significantly improve the lifetime of the BEC in a rotating field.

In summary, we realized a scheme to tune the averaged DDI strength in a dipolar BEC. This was accomplished by rapidly rotating a magnetic field. We demonstrate that the AR of the BEC after long TOF can be tuned from 2.3 to below unity, confirming the expectation from Eq. (1), introduced in Ref. [34], that both the magnitude and sign of the DDI can be tuned by rotating the dipoles at different angles φ. Furthermore, at the magic rotation angle $\varphi_m = 54.7°$, expansion dynamics of our dysprosium BEC is similar to that of a non-dipolar gas, demonstrating that the DDI can be nearly turned off in rotating fields. This work shows that a new tool—the tuning of the DDI, and consequently, ϵ—is readily available to control atomic interactions for the propose of creating exotic quantum many-body systems.

We acknowledge support from AFOSR (FA9550-17-1-0266) and NSF (PHY-1707336). WK acknowledges support from NSERC Postgraduate Scholarship-Doctoral.

[1] M. Lu, N. Q. Burdick, S. H. Youn, and B. L. Lev, "Strongly dipolar Bose-Einstein condensate of dysprosium," Phys. Rev. Lett. **107**, 190401 (2011).
[2] M. Lu, N. Q. Burdick, and B. L. Lev, "Quantum degenerate dipolar fermi gas," Phys. Rev. Lett. **108**, 215301 (2012).
[3] K. Aikawa, A. Frisch, M. Mark, S. Baier, A. Rietzler, R. Grimm, and F. Ferlaino, "Bose-Einstein condensation of erbium," Phys. Rev. Lett. **108**, 210401 (2012).
[4] K. Aikawa, A. Frisch, M. Mark, S. Baier, R. Grimm, and F. Ferlaino, "Reaching fermi degeneracy via universal dipolar scattering," Phys. Rev. Lett. **112**, 010404 (2014).
[5] H. Kadau, M. Schmitt, M. Wenzel, C. Wink, T. Maier, I. Ferrier-Barbut, and T. Pfau, "Observing the Rosensweig instability of a quantum ferrofluid," Nature **530**, 194–197 (2016).
[6] M. Schmitt, M. Wenzel, F. Böttcher, I. Ferrier-Barbut, and T. Pfau, "Self-bound droplets of a dilute magnetic quantum liquid," Nature **539**, 259–262 (2016).
[7] L. Chomaz, S. Baier, D. Petter, M. J. Mark, F. Wächtler, L. Santos, and F. Ferlaino, "Quantum-fluctuation-driven crossover from a dilute Bose-Einstein condensate to a macrodroplet in a dipolar quantum fluid," Phys. Rev. X **6**, 041039 (2016).
[8] I. Ferrier-Barbut, H. Kadau, M. Schmitt, M. Wenzel, and T. Pfau, "Observation of quantum droplets in a strongly dipolar bose gas," Phys. Rev. Lett. **116**, 215301 (2016).
[9] A. de Paz, A. Sharma, A. Chotia, E. Maréchal, J. H. Huckans, P. Pedri, L. Santos, O. Gorceix, L. Vernac, and B. Laburthe-Tolra, "Nonequilibrium Quantum Magnetism in a Dipolar Lattice Gas," Phys. Rev. Lett. **111**, 185305 (2013).
[10] A. de Paz, P. Pedri, A. Sharma, M. Efremov, B. Naylor, O. Gorceix, E. Maréchal, L. Vernac, and B. Laburthe-Tolra, "Probing spin dynamics from the Mott insulating to the superfluid regime in a dipolar lattice gas," Phys. Rev. A **93**, 021603 (2016).
[11] S. Baier, M. J. Mark, D. Petter, K. Aikawa, L. Chomaz, Z. Cai, M. Baranov, P. Zoller, and F. Ferlaino, "Extended Bose-Hubbard models with ultracold magnetic atoms," Science **352**, 201 (2016).
[12] B. Naylor, M. Brewczyk, M. Gajda, O. Gorceix, E. Maréchal, L. Vernac, and B. Laburthe-Tolra, "Competition between Bose-Einstein condensation and spin dynamics," Phys. Rev. Lett. **117**, 185302 (2016).
[13] S. Lepoutre, J. Schachenmayer, L. Gabardos, B. Zhu, B. Naylor, E. Maréchal, O. Gorceix, A. M. Rey, L. Vernac, and B. Laburthe-Tolra, "Exploring out-of-equilibrium quantum magnetism and thermalization in a spin-3 many-body dipolar lattice system," arXiv:1803.02628 (2018).
[14] Y. Tang, W. Kao, K. Li, S. Seo, K. Mallayya, M. Rigol, S. Gopalakrishnan, and B. L. Lev, "Thermalization near integrability in a dipolar quantum Newton's cradle," (2018), arXiv:1707.07031; to appear in PRX.
[15] P. Pedri and L. Santos, "Two-dimensional bright solitons in dipolar Bose-Einstein condensates," Phys. Rev. Lett. **95**, 200404 (2005).
[16] R. Nath, P. Pedri, and L. Santos, "Stability of dark solitons in three dimensional dipolar Bose-Einstein con-

densates," Phys. Rev. Lett. **101**, 210402 (2008).
[17] T. Lahaye, C. Menotti, L. Santos, M. Lewenstein, and T. Pfau, "The physics of dipolar bosonic quantum gases," Rep. Prog. Phys. **72**, 126401 (2009).
[18] B. C. Mulkerin, R. M. W. van Bijnen, D. H. J. O'Dell, A. M. Martin, and N. G. Parker, "Anisotropic and long-range vortex interactions in two-dimensional dipolar bose gases," Phys. Rev. Lett. **111**, 170402 (2013).
[19] M. Klawunn, R. Nath, P. Pedri, and L. Santos, "Transverse instability of straight vortex lines in dipolar Bose-Einstein condensates," Phys. Rev. Lett. **100**, 240403 (2008).
[20] N. R. Cooper, E. H. Rezayi, and S. H. Simon, "Vortex lattices in rotating atomic bose gases with dipolar interactions," Phys. Rev. Lett. **95**, 200402 (2005).
[21] R. W. Cherng and E. Demler, "Magnetoroton softening in rb spinor condensates with dipolar interactions," Phys. Rev. Lett. **103**, 185301 (2009).
[22] L. He, J. N. Zhang, Y. Zhang, and S. Yi, "Stability and free expansion of a dipolar fermi gas," Phys. Rev. A **77**, 031605 (2008).
[23] B. M. Fregoso, K. Sun, E. Fradkin, and B. L. Lev, "Biaxial nematic phases in ultracold dipolar fermi gases," New J. Phys. **11**, 103003–8 (2009).
[24] J. N. Zhang and S. Yi, "Fermi surface of a trapped dipolar fermi gas," Phys. Rev. A **80**, 053614 (2009).
[25] K. Aikawa, S. Baier, A. Frisch, M. Mark, C. Ravensbergen, and F. Ferlaino, "Observation of fermi surface deformation in a dipolar quantum gas," Science **345**, 1484 (2014).
[26] S. Sinha and L. Santos, "Cold dipolar gases in quasi-one-dimensional geometries," Phys. Rev. Lett. **99**, 140406 (2007).
[27] R. Citro, E. Orignac, S. De Palo, and M. L. Chiofalo, "Evidence of Luttinger-liquid behavior in one-dimensional dipolar quantum gases," Phys. Rev. A **75**, 051602 (2007).
[28] S. Yi, T. Li, and C. P. Sun, "Novel quantum phases of dipolar bose gases in optical lattices," Phys. Rev. Lett. **98**, 260405 (2007).
[29] M. Hafezi, A. S. Sørensen, E. Demler, and M. D. Lukin, "Fractional quantum Hall effect in optical lattices," Phys. Rev. A **76**, 023613 (2007).
[30] B. Liu, X. Li, L. Yin, and W. V. Liu, "Weyl Superfluidity in a three-dimensional dipolar fermi gas," Phys. Rev. Lett. **114**, 045302 (2015).
[31] S.-Y. Chä and U. R. Fischer, "Probing the scale invariance of the inflationary power spectrum in expanding quasi-two-dimensional dipolar condensates," Phys. Rev. Lett. **118**, 130404 (2017).
[32] M. Fattori, G. Roati, B. Deissler, C. D'Errico, M. Zaccanti, M. Jona-Lasinio, L. Santos, M. Inguscio, and G. Modugno, "Magnetic dipolar interaction in a Bose-Einstein condensate atomic interferometer," Phys. Rev. Lett. **101**, 190405 (2008).
[33] G. Baym and T. Hatsuda, Private communication.
[34] S. Giovanazzi, A. Görlitz, and T. Pfau, "Tuning the dipolar interaction in quantum gases," Phys. Rev. Lett. **89**, 130401 (2002).
[35] Reducing the DDI through "magic angle rotation" has been discussed in the NMR context [52].
[36] C. Chin, R. Grimm, P. Julienne, and E. Tiesinga, "Feshbach resonances in ultracold gases," Rev. Mod. Phys. **82**, 1225 (2010).
[37] Control of ϵ via a Feshbach resonance is often difficult in many highly magnetic atomic isotopes due to the narrowness of the resonances [53].
[38] We chose ^{162}Dy over ^{164}Dy, despite the greater isotopic abundance of ^{164}Dy, due to the fact that we can produce more populous BECs of ^{162}Dy. This is because of its more favorable ratio of dipolar length to s-wave scattering length; see Ref. [42].
[39] S. Hensler, J. Werner, A. Griesmaier, P. O. Schmidt, A. Görlitz, T. Pfau, S. Giovanazzi, and K. Rzażewski, "Dipolar relaxation in an ultra-cold gas of magnetically trapped chromium atoms," Applied Physics B **77**, 765 (2003).
[40] B. Pasquiou, G. Bismut, Q. Beaufils, A. Crubellier, E. Maréchal, P. Pedri, L. Vernac, O. Gorceix, and B. Laburthe-Tolra, "Control of dipolar relaxation in external fields," Phys. Rev. A **81**, 042716 (2010).
[41] N. Q. Burdick, K. Baumann, Y. Tang, M. Lu, and B. L. Lev, "Fermionic Suppression of Dipolar Relaxation," Phys. Rev. Lett. **114**, 023201 (2015).
[42] Y. Tang, N. Q. Burdick, K. Baumann, and B. L. Lev, "Bose–Einstein condensation of ^{162}Dy and ^{160}Dy," New J. Phys. **17**, 045006 (2015).
[43] The error in this number is quoted as the worst case error. This worst case occurs at $\varphi = 90°$, since the uncertainty in $B_{\rm rot}$ is larger than in B_z.
[44] K. Baumann, N. Q. Burdick, M. Lu, and B. L. Lev, "Observation of low-field Fano-Feshbach resonances in ultracold gases of dysprosium," Phys. Rev. A **89**, 020701 (2014).
[45] W. C. Martin, R. Zalubas, and L. Hagan, *Atomic Energy Levels–The Rare Earth Elements* (NSRDS-NBS, **60**, Washington, D.C., 1978).
[46] S. Giovanazzi, P. Pedri, L. Santos, A. Griesmaier, M. Fattori, T. Koch, J. Stuhler, and T. Pfau, "Expansion dynamics of a dipolar Bose-Einstein condensate," Phys. Rev. A **74**, 013621 (2006).
[47] Y. Castin and R. Dum, "Bose-Einstein condensates in time dependent traps," Phys. Rev. Lett. **77**, 5315 (1996).
[48] D. H. J. O'Dell, S. Giovanazzi, and C. Eberlein, "Exact hydrodynamics of a trapped dipolar bose-einstein condensate," Phys. Rev. Lett. **92**, 250401 (2004).
[49] C. Eberlein, S. Giovanazzi, and D. H. J. O'Dell, "Exact solution of the Thomas-Fermi equation for a trapped Bose-Einstein condensate with dipole-dipole interactions," Phys. Rev. A **71**, 033618 (2005).
[50] Y. Tang, A. G. Sykes, N. Q. Burdick, J. M. DiSciacca, D. S. Petrov, and B. L. Lev, "Anisotropic expansion of a thermal dipolar bose gas," Phys. Rev. Lett. **117**, 155301 (2016).
[51] That is, any rotation rate lower than a few hundred Hz decreased the BEC lifetime. We were unable to measure lifetimes at rotation rates faster than ∼1 kHz due to power supply limitations and increasingly large eddy currents. We typically used 1-kHz rotation rates to ensure as large a separation in frequency as possible between this rate and the trap frequencies.
[52] M. M. Maricq and J. S. Waugh, "NMR in rotating solids," J. Chem. Phys. **70**, 3300–3316 (1979).
[53] S. Kotochigova, "Controlling interactions between highly magnetic atoms with Feshbach resonances," Rep. Prog. Phys. **77**, 093901 (2014).